Available online at www.sciencedirect.com

SCIENCE DIRECT

Virology 325 (2004) 351–363

VIROLOGY

www.elsevier.com/locate/yviro

Complete genomic DNA sequence of rock bream iridovirus

Jeong Wan Do,[a] Chang Hoon Moon,[b] Hyo Jeong Kim,[b] Myoung Seok Ko,[b] Sung Bum Kim,[b] Ji Hee Son,[b] Jong Soo Kim,[b] Eun Jeong An,[b] Min Kyoung Kim,[b] Seung Koo Lee,[b] Myung Shin Han,[b] Seung Ju Cha,[b] Mi Seon Park,[a] Myoung Ae Park,[a] Yi Cheong Kim,[a] Jin Woo Kim,[a] and Jeong Woo Park[b,*]

[a] *Pathology Division, National Fisheries Research and Development Institute, Kijang, Pusan 626-900, South Korea*
[b] *Department of Biological Sciences, University of Ulsan, Ulsan 680-749, South Korea*

Received 3 February 2004; returned to author for revision 22 March 2004; accepted 5 May 2004
Available online 17 June 2004

Abstract

Iridovirus is a causative agent of epizootics among cultured rock bream (*Oplegnathus fasciatus*) in Korea. Here, we report the complete genomic sequence of rock bream iridovirus (RBIV). The genome of RBIV was 112 080 bp long and contained at least 118 putative open reading frames (ORFs), and its genome organization was similar to that of infectious spleen and kidney necrosis virus (ISKNV). Of the RBIV's 118 ORFs, 85 ORFs showed 60–99% amino acid identity to those of ISKNV. Phylogenetic analysis of major capsid protein (MCP), DNA repair protein RAD2, and DNA polymerase type-B family indicated that RBIV is closely related to red sea bream iridovirus (RSIV), Grouper sleepy disease iridovirus (GSDIV), Dwarf gourami iridovirus (DGIV), and ISKNV. The genome sequence provides useful information concerning the evolution and divergence of iridoviruses in cultured fish.

Keywords: RBIV; Iridovirus; Genome

Introduction

Iridoviruses are large cytoplasmic DNA viruses with an icosahedral morphology (Williams, 1996). The genome is both circularly permutated and terminally redundant, which is a unique feature among eukaryotic virus genomes (Goorha and Murti, 1982). Based on the index of viruses database of the International Committee on Taxonomy of Viruses (ICTVdB) (http://www.ncbi.nlm. nih.gov/ICTVdb/Ictv/index.htm), the Iridoviridae family is subdivided into four genera including Iridovirus, Chloriridovirus, Ranavirus, and Lymphocystivirus. Currently, five entire genomes of iridoviruses, such as lymphocystis disease virus 1 (LCDV-1, the type species of the genus Lymphocystivirus; Tidona and Darai, 1997; accession no. L63545), Chilo iridescent virus (CIV, the type species of the genus of Iridovirus; Jakob et al., 2001; accession no. AF303741), infectious spleen and kidney necrosis virus (ISKNV; He et al., 2001; accession no. AF371960), tiger frog virus (TFV; He et al., 2002; accession no. AF389451), and Ambystoma tigrinum virus (ATV; Jancovich et al., 2003; accession no. AY150217) have been fully characterized.

Iridoviruses infect a wide variety of cultured fish (Hetrick and Hedrick, 1993; Wolf, 1988). According to the ICTVdB, most fish iridoviruses are members either of the genus Lymphocystivirus or of the genus Ranavirus. While iridoviruses belonging to the genus Lymphocystivirus cause the development of clusters of extremely hypertrophied fibroblasts or osteoblasts called lymphocystis cells, other iridoviruses belonging to the genus Ranavirus cause systemic disease in infected animals and are associated with high morbidity and mortality (Ahne et al., 1989; Hedrick and McDowell, 1995; Hedrick et al., 1992; Langdon et al., 1986; Pozet et al., 1992). However, taxonomic analysis of the putative proteins suggests the presence of fish iridoviruses which belong neither to the genus Ranavirus nor to the genus Lymphocystivirus (He et al., 2001; Hyatt et al., 2000).

Recently, iridoviral epizootics have occurred frequently among cultured fish in Korea (Jung and Oh, 2000; Kim et al., 2002) and, especially, iridoviral disease has caused

* Corresponding author. Fax: +82-52-259-1694.
E-mail address: jwpark@uou.ulsan.ac.kr (J.W. Park).

0042-6822/$ - see front matter © 2004 Elsevier Inc. All rights reserved.
doi:10.1016/j.virol.2004.05.008

severe damage to rock bream (*Oplegnathus fasciatus*) cultures in Korea. Here, we report the characterization of the rock bream iridovirus (RBIV) genome by DNA sequencing and we compare the genome structure with that of other iridoviruses such as LCDV-1 and ISKNV. Based on a phylogenetic analysis of putative protein, we also discuss the taxonomic position of RBIV.

Results and discussion

Determination of the viral genomic DNA sequence

PCR was performed to amplify the complete genomic DNA of RBIV. Recently, a complete genomic DNA sequence of ISKNV, an iridovirus from mandarin fish, was reported (He et al., 2001) and we found that the nucleotide sequences of ATPase and MCP of RBIV showed 97% and 98% identities with those of ISKNV, respectively (data not shown). Thus, primers for PCR were designed from nucleotide sequences in the GenBank/EMBL/DDBJ and NCBI nucleotide sequence databases of ISKNV (AF371960). More than overlapping 120 PCR primer pairs were designed so that the average PCR product ranged from 1000 to 1200 bp. The PCR products were cloned into pGEMt vector and the nucleotide sequence of the cloned DNA fragments was determined by using M13 forward and M13 reverse sequencing primers in the vector and more than 240 internal sequencing primers. Every nucleotide position in the viral genome was determined more than once from each DNA strand. The average read length obtained from individual sequencing reactions ranged from 600 to 800 nucleotides.

The complete RBIV genome was 112 080 bp, which was 718 bp larger than that of ISKNV (111 362 bp) (He et al., 2001). The GC content of the RBIV genome was 53%, which was similar to that of ISKNV (54.78%) (He et al., 2001), TFV (55.01%) (He et al., 2002), and ATV (54%) (Jancovich et al., 2003), but significantly higher than that of LCDV-1 (29.07%) (Tidona and Darai, 1997) and CIV (28.63%) (Jakob et al., 2001) (Table 1).

Coding capacity of the RBIV genome

A computer-assisted analysis of the complete DNA sequence of RBIV identified 118 potential nonoverlapping open reading frames (ORFs) with coding capacities for polypeptides ranging from 50 to 1253 amino acids (Fig. 1, Table 2). The potential ORFs detected within the nucleotide sequences of the upper (R) and lower (L) DNA strands were consecutively numbered as listed in Table 2 and a diagrammatic representation of the RBIV genome is shown in Fig. 1. An analysis of the amino acid sequences deduced from the individual ORFs revealed 29 ORFs with significant homology to functionally characterized proteins of other species and 31 ORFs of unknown function with no homology to other iridovirus sequences (Fig. 1, Table 2).

Comparison to other iridoviruses isolated from fish

Originally, PCR primers for the amplification of RBIV genomic DNA were designed based on the nucleotide sequences of ISKNV (He et al., 2001). Thus, we, first, compared the complete genome sequence of RBIV to the sequence data of ISKNV in GenBank. RBIV is highly similar to ISKNV at the genomic level, sharing colinearity (85 orthologous genes). Among the 118 ORFs, the proteins encoded by 85 ORFs showed 60–99% amino acid identity to proteins from ISKNV. Of the 85 ORFs, RBIV and ISKNV share 53, 25, and 7 genes with 91–99%, 81–90%, and 60–80% amino acid identity, respectively (Table 2). Of the seven least similar ORFs, six (ORF004L, ORF065L, ORF099L, ORF100R, ORF110R, and ORF115L) showed no homology to functionally characterized proteins in databases but ORF023R had a laminin-type epidermal growth factor-like domain and likely plays some role in host-related functions.

Of the 85 ORFs, 54 RBIV ORFs differ from ISKNV ORFs in size due to an insertion or deletion of amino acids within the ORF or an alteration in start or stop codons. The most dramatic size differences were found in five RBIV ORFs, such as ORF103R, ORF105L, ORF106L, ORF108R, and ORF109R. ORF105L and ORF106L of RBIV are a fragmented form of ISKNV ORF114L. ORF105L (523 aa) and ORF106L (358 aa) of RBIV encode homologues of the C-terminal and N-terminal region of a protein encoded by the ORF114L (941 aa) of ISKNV, respectively. Similarly, ORF108R and ORF109R of RBIV are a fragmented form of ISKNV ORF115R. ORF108R (243 aa) and ORF109R (77 aa) of RBIV encode homologues of the C-terminal and N-terminal region of a protein encoded by the ORF115R (336 aa) of ISKNV, respectively. ORF103R encoded 146-amino-acid protein which is homologous to the N-terminus of

Table 1
Summary of genomic information for six viral species within the family Iridoviridae

Genus	Iridovirus	Ranavirus	Ranavirus	Lymphocystivirus	Unassigned	Unassigned
Species	CIV	ATV	TFV	LCDV-1	ISKNV	RBIV
Genome size (bp)	212 482	106 332	105 057	102 653	111 362	112 080
GC (%)	28.6	54	55	29.1	54.8	53
No. putative ORFs	468	96	105	195	124	118
ORF size (aa)	40–2432	32–1294	40–1294	40–1199	40–1208	50–1253
Accession no.	AF303741	AY150217	NC003407	NC001824	NC003494	AY532606

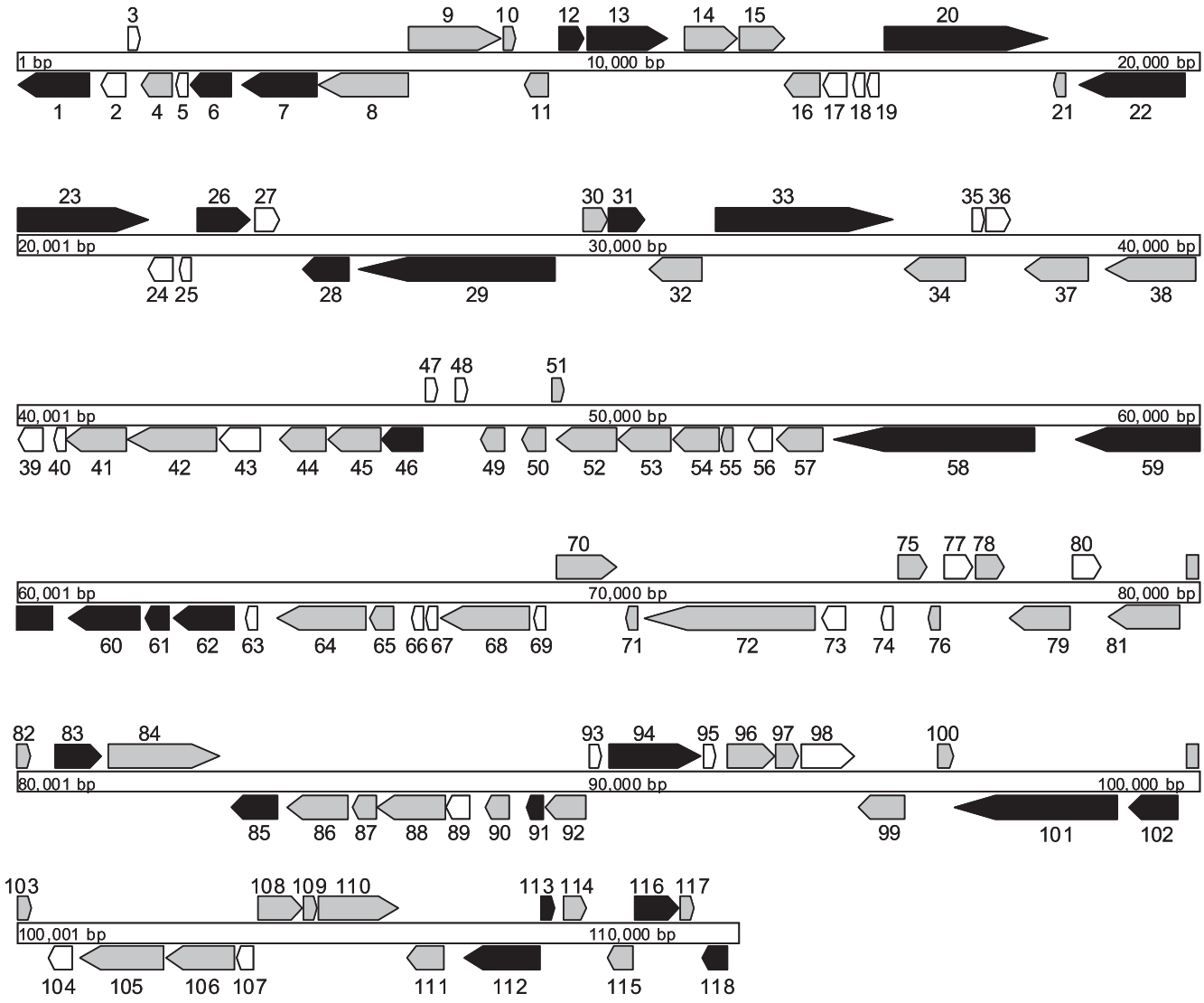

Fig. 1. RBIV genome organization. Predicted ORFs are depicted by arrows with spearheads pointing in the direction of transcription. ORFs of predicted function with homology to other iridoviral ORFs are drawn in black and ORFs of unknown function with homology with other iridoviral ORFs are in grey, while ORFs of unknown function with no homology to other iridoviral ORFs are in white.

ISKNV ORF112R (247 aa). It is not likely that the size difference and fragmentation result in functional inactivation and, thus, affect viral virulence because both ISKNV and RBIV are highly virulent to mandarin fish and rock fish, respectively. This result suggests that gene fragmentation and sequence divergence occurred during the adaptation of the iridovirus to rock bream and mandarin fish.

Next, the genome of the RBIV was compared to the 10 ORFs of RSIV available in the GenBank. Ten ORFs of the RBIV are more similar to those of the RSIV (90–99% amino acid sequence identity) than to those of the ISKNV (72–98% identity). However, we found some differences between RBIV and RSIV. Of the 10 ORFs, 5 ORFs are different in size between RBIV and RSIV. Especially, the sizes of ORF009R (515 aa) and ORF023R (805 aa) of RBIV are significantly different from homologues of RSIV [accession nos.: BAC66966 (377 aa) and AAQ07956 (1050 aa)].

Sequence similarities to proteins in the databases

The deduced translation products of the 118 ORFs were compared to amino acid sequences in GenBank. Thirty-two ORFs showed significant homology to functionally characterized proteins of other species and these proteins included enzymes and structural proteins involved in virus replication, transcription, protein modification, and virus–host interaction (Table 2).

Proteins involved in DNA replication, modification, and processing

Most large DNA viruses encode a set of genes involved in DNA replication, repair, and nucleotide metabolism, enabling their efficient replication in host cells (Reichard, 1988). Similarly, RBIV ORFs encoded DNA polymerase

Table 2
RBIV ORFs

ORF	Position	Length (aa)[a]	Predicted structure and/or function[b]	Best match				ISKNV			RSIV[c]		LCDV-1		
				Species	Accession no.[d]	BlastP score	%Id	ORF[e]	Length (aa)[a]	%Id	Length (aa)[a]	%Id	ORF[f]	Length (aa)[a]	%Id
001L	134–1270	378	Aa_trans, transmembrane Amino acid transporter protein	ISKNV	NP_612223	486	95	001L	378	95					
002L	1391–1699	102													
003R	1841–2056	71													
004L	2102–2605	167		ISKNV	NP_612225	226	77	003L	185	77					
005L	2624–2800	58													
006L	2876–3541	221	CPDc, catalytic domain of ctd-ike phosphatases	ISKNV	NP_612227	424	95	005L	251	95			082L	176	33
007L	3786–5147	453	major capsid protein	RSIV	NP_612228	856	99	006L	453	98	453	99	147L	459	46
008L	5164–6621	485		RSIV	NP_612229	813	99	007L	485	97	485	99	067L	459	29
009R	6692–8239	515		ISKNV	NP_612230	924	89	008R	525	89	377	93			
010R	8335–8496	53		ISKNV	NP_612231	59	92	009R	53	92					
011L	8655–9047	130		ISKNV	NP_612232	243	94	010L	130	94					
012R	9323–9655	110	RING-finger-containing ubiquitin ligase	ISKNV	NP_612234	196	97	012R	110	97					
013R	9662–11059	465	serine/Threonine protein kinase, catalytic domain	ISKNV	NP_612235	833	89	013R	461	89			143L	467	25
014R	11314–12288	324		ISKNV	NP_612236	572	95	014R	319	95					
015R	12298–13089	263		ISKNV	NP_612237	454	95	015R	263	95					
016L	13146–13733	195		ISKNV	NP_612238	341	91	016L	195	91					
017L	13748–14086	112													
018L	14171–14410	79													
019L	14472–14648	58													
020R	14664–17510	948	DNA polymerase type-B family	ISKNV	NP_612241	1933	97	019R	948	97	947	97	135R	932	35
021L	17574–17756	60		ISKNV	NP_612242	60	87	020L	62	87					

022L	18104–19714	536	Predicted phosphatase	RSIV	AAQ07955	877	94	022L	499	92	531	94			
023R	19787–22204	805	laminin-type epidermal growth factor-like domain	RSIV	AAQ07956	963	90	023R	856	72	1050	90			
024L	22346–22657	103													
025L	22847–22999	50													
026R	23035–23973	312	ribonucleotide reductase, small chain	RSIV	BAA82755	624	98	024R	312	96	312	98			
027R	23997–24380	127													
028L	24719–25615	298	DNA repair protein RAD2	RSIV	BAA82754	559	98	027L	298	97	298	98	191R	333	30
029L	25632–29138	1168	RNA polymerase beta subunit	RSIV	BAA82753	2384	97	028L	1159	95	1159	97	016L	1199	36
030R	29653–29895	80		ISKNV	NP_612253	116	85	031R	80	85					
031R	29990–30622	210	deoxyribonucleoside kinase	ISKNV	NP_612254	365	88	032R	204	88					
032L	30713–31654	313		ISKNV	NP_612255	540	88	033L	313	88					
033R	31700–34861	1053	RNA polymerase beta subunit	ISKNV	NP_612256	2091	95	034R	1044	95			025L	1024	43
034L	34934–36067	377		ISKNV	NP_612257	676	88	035L	382	88					
035R	36069–36242	57													
036R	36422–36679	91													
037L	37110–38219	369		ISKNV	NP_612259	645	90	037L	450	90					
038L	38469–39974	501		ISKNV	NP_612260	783	86	038L	478	86					
039L	40008–40307	99													
040L	40632–40802	56													
041L	40850–41995	381		ISKNV	NP_612262	646	88	040L	379	88					
042L	41997–43346	449		ISKNV	NP_612263	685	87	041L	447	87					
043L	43523–44140	205													
044L	44408–45208	266		ISKNV	NP_612266	457	87	044L	266	87					
045L	45213–46127	304		ISKNV	NP_612267	490	87	045L	304	87					
046L	46121–46804	227	cytosine DNA methyl transferase	ISKNV	NP_612268	419	96	046L	227	96			005L	228	43
047R	46887–47150	87													
048R	47369–47620	83													
049L	47842–48270	142		ISKNV	NP_612272	268	90	050L	142	90					
050L	48547–48999	150		ISKNV	NP_612274	237	82	052L	150	82					
051R	49001–49195	64		ISKNV	NP_612275	88	89	053R	71	89					
052L	49229–50173	314		ISKNV	NP_612276	459	92	054L	308	92					
053L	50196–51137	313		ISKNV	NP_612277	419	92	055L	308	92					
054L	51148–51795	215		ISKNV	NP_612278	336	98	056L	215	98					
055L	51802–52062	86		ISKNV	NP_612279	160	95	057L	86	95					

(*continued on next page*)

Table 2 (*continued*)

ORF	Position	Length (aa)[a]	Predicted structure and/or function[b]	Best match				ISKNV			RSIV[c]		LCDV-1		
				Species	Accession no.[d]	BlastP score	%Id	ORF[e]	Length (aa)[a]	%Id	Length (aa)[a]	%Id	ORF[f]	Length (aa)[a]	%Id
056L	52327–52839	170													
057L	52903–53709	268		ISKNV	NP_612283	478	90	061L	267	90					
058L	53706–57467	1253	predicted DNA-binding protein, contains SAP domain	ISKNV	NP_612284	1899	89	062L	1208	89					
059L	57919–60567	882	SNF2 family helicase	ISKNV	NP_612285	1725	95	063L	882	95			132L	944	31
060L	60855–62102	415	mRNA capping enzyme	ISKNV	NP_612286	716	95	064L	491	95					
061L	62144–62611	155	RING-finger-containing E3 ubiquitin ligase	ISKNV	NP_612287	215	94	065L	153	94					
062L	62662–63744	360	RING-finger-containing	E3 ubiquitin ligase ISKNV	NP_612288	556	87	066L	347	87					
063L	63896–64129	77													
064L	64484–65917	477		ISKNV	NP_612290	873	94	068L	477	94					
065L	65929–66435	168		ISKNV	NP_612291	108	60	069L	221	60					
066L	66680–66907	75													
067L	66913–67086	57													
068L	67120–68529	469		ISKNV	NP_612293	870	92	071L	536	92					
069L	68717–68941	74													
070R	69184–70203	339		ISKNV	NP_612296	622	90	074R	337	90					
071L	70304–70573	89		ISKNV	NP_612297	78	92	075L	88	92					
072L	70575–73541	988		ISKNV	NP_612298	1887	94	076L	990	94			163R	1085	22
073L	73621–73971	116													
074L	74606–74839	77													
075R	74890–75354	154		ISKNV	NP_612300	275	96	078R	154	96					
076L	75356–75580	74		ISKNV	NP_612301	99	94	079L	73	94					
077R	75664–76137	157													
078R	76150–76647	165		ISKNV	NP_612303	285	98	081R	165	98					
079L	76696–77802	368		ISKNV	NP_612304	716	94	082L	368	94					
080R	77827–78225	132													
081L	78252–79556	434		ISKNV	NP_612306	805	90	084L	451	90					
082R	79643–80173	176		ISKNV	NP_612307	166	86	085R	200	86					
083R	80603–81400	265	dsRNA-specific ribonuclease	ISKNV	NP_612309	501	97	087R	256	97			137R	251	29

084R	81503–83425	640		ISKNV	NP_612310	1102	91	088R	667	91					
085L	83630–84457	275	membrane (myristylated) protein	LCDV-1	NP_078745	121	33						160L	344	33
086L	84578–85504	308		ISKNV	NP_612315	484	93	093L	308	93					
087L	85514–86014	166		ISKNV	NP_612316	282	96	094L	166	96					
088L	86039–87202	387		ISKNV	NP_612317	639	93	095L	386	93					
089L	87218–87601	127													
090L	87952–88443	163		LCDV-1	NP_078659	34	25						059L	153	25
091L	88491–88814	107	RING-finger domain	ISKNV	NP_612321	167	91	099L	107	91					
092L	88868–89515	215		ISKNV	NP_612322	303	86	100L	181	86					
093R	89653–89820	55													
094R	90068–91513	481	ankyrin repeats	ISKNV	NP_612324	909	91	102R	480	91					
095R	91520–91774	84													
096R	91994–92773	259		ISKNV	NP_612326	470	89	104R	258	89					
097R	92775–93146	123		ISKNV	NP_612327	220	95	105R	121	95					
098R	93240–94127	295													
099L	94221–95042	273		ISKNV	NP_612328	399	76	106L	339	76					
100R	95486–95770	94		ISKNV	NP_612330	60	77	108R	49	77					
101L	95792–98557	921	predicted ATPase	ISKNV	NP_612331	1866	97	109L	921	97			128L	874	34
102L	98761–99657	298	Tnf receptor associated factor 2 domain	ISKNV	NP_612333	530	93	111L	296	93					
103R	99677–100117	146		ISKNV	NP_612334	276	99	112R	247	99			003L	248	35
104L	100423–100914	163													
105L	100953–102524	523		ISKNV	NP_612336	998	91	114L	941 (439–941)	91			195R	935	23
106L	102539–103615	358		ISKNV	NP_612336	682	96	114L	941 (82–412)	96					
107L	103639–103941	100													
108R	104050–104781	243		ISKNV	NP_612337	414	84	115R	336 (1–243)	84			047L	374	33
109R	104821–105054	77		ISKNV	NP_612337	152	94	115R	336 (260–336)	94					
110R	105060–106493	477		ISKNV	NP_612339	634	75	116R	482	75					
111L	106547–107221	224		ISKNV	NP_612340	449	95	117L	224	95					
112L	107549–108913	454	ankyrin repeats	ISKNV	NP_612341	820	92	118L	456	92					
113R	108931–109104	57	RING-finger-containing	E3 ubiquitin ligase ISKNV	NP_612342	86	92	119R	95	92					
114R	109248–109637	129		ISKNV	NP_612343	199	92	120R	169	92					
115L	109970–110419	149		ISKNV	NP_612344	201	74	121L	216	74					
116R	110429–111148	239	adenosine triphosphatase	RSIV	BAA28670	504	99	122R	239	98	239	99	054R	244	53
117R	111226–111420	64		ISKNV	NP_612346	82	95	123R	61	95					
118L	111576–112037	153	putative ankyrin repeat protein	ISKNV	NP_612347	256	94	124L	228	94					

[a] aa = amino acids.
[b] Function was deduced either from the degree of similarity to known genes or from the presence of Prosite signatures.
[c] Best-matching ORF from the RSIV genes.
[d] Accession numbers are from GenBank.
[e] Best-matching ORF from the ISKNV genome (accession no. AF371960).
[f] Best-matching ORF from the LCDV-1 genome (accession no. L63545).

(ORF020R), DNA repair protein RAD2 (ORF028L), deoxyribonucleoside kinase (ORF031R), cytosine DNA methyltransferase (ORF046L), and helicase (ORF059L). DNA polymerase, DNA repair protein RAD2, cytosine DNA methyltransferase, and helicase are highly conserved between RBIV and ISKNV: their sizes are the same and they showed 95–97% amino acid sequence identity. However, interestingly, the deoxyribonucleoside kinase is less conserved: their size is different and they showed 88% amino acid sequence identity. Especially the N-terminal showed very low similarity. Deoxyribonucleoside kinases catalyze the phosphorylation of deoxyribonucleosides (dN) to the corresponding deoxyribonucleoside monophosphates (dNMP). They are the key enzymes in the salvage of dN originating from the extra- or intracellular breakdown of DNA. Subsequently, dNMPs are phosphorylated into diphosphates and triphosphates, which are the precursors of DNA. Recent studies on the structure–function relationship revealed that residues in the middle core region of deoxyribonucleoside kinase are involved in substrate specificity (Johansson et al., 2001; Knecht et al., 2000). Thus, it is not likely that the difference in the N-terminal region provides the structural basis for the different substrate specificity of the dNKs. It is possible that this N-terminal region plays some role in interaction with other cellular proteins and different structures may be required for the interaction with proteins in different species.

Transcription and nucleotide metabolism

RBIV encode at least five enzymes which are involved in transcription and nucleotide metabolism. They are ribonucleotide reductase beta subunit (ORF026R), beta subunit/160-kDa subunit of the DNA-dependent RNA polymerase (RpoC) (ORF029L), beta subunit/140-kDa subunit of DNA-dependent RNA polymerase (RpoB) (ORF033R), mRNA capping enzyme (ORF060L), and dsRNA-specific ribonuclease (ORF083R). These genes of RBIV are similar to those found in ISKNV and they showed 95–98% amino acid sequence identities.

Protein modification and host-related functions

RBIV encode at least 14 proteins involved in protein modification or host-related functions.

ORF006L encodes a protein of 221 amino acids which showed homology to the C-terminal domain (CTD)-like phosphatase. CTD phosphatase is specific for RNA polymerase II and removes phosphates from the CTD. CTD phosphatase acting on free RNA polymerase II increases the pool of RNAP II available for initiation thereby acting as an activator of transcription (O'Brien et al., 1994). This suggests that the product of ORF006L may act as an activator of transcription by acting on free iridoviral RNA polymerase.

ORF012R, 061L, 062L, 091L, and 113R encoded proteins of various sizes which contain RING-finger-containing ubiquitin ligase domain. A viral protein of herpes simplex virus type 1 (HSV-1), called ICP0, contains RING-finger domain and this region in ICP0 is essential for its functions in regulating gene expression, stimulating lytic infection and reactivation from quiescence, disruption of ND10 and centromeres, induced proteasome-dependent degradation of cellular proteins, interaction with cyclin D3, and induction of colocalizing, conjugated ubiquitin (Everett, 1988, 2000). Similarly, the five RBIV proteins containing RING-finger domain may have some essential functions in viral replication. All the five proteins possessed the 'cross-brace' motif C-X2-C-X(9-39)-C-X(1-3)-H-X(2-3)-(N/C/H)-X2-C-X(4-48)C-X2-C, which is probably involved in mediating protein–protein interactions. Outside this motif, they showed no homology, suggesting that they may control different pathways during virus replication.

ORF013R encoded a protein of 465 amino acids which showed homology to the serine/threonine protein kinase. Herpes simplex virus type 1 encodes a serine/threonine kinase (UL13) that is packaged into the virion (Cunningham et al., 1992; Overton et al., 1992). UL13 seems to play an important role in various stages of the HSV-1 life cycle including the viral penetration of cells and the onset of viral protein synthesis by phosphorylating target proteins. Similarly, ORF013R may phosphorylate viral proteins or cellular protein and regulate virus infection and viral gene expression.

ORF022R encoded a protein of 805 amino acids and this contained a laminin-type epidermal growth factor-like domain. Laminins are the major noncollagenous components of basement membrane assembly that mediate cell adhesion, growth migration, and differentiation. Nidogen, an invariant component of basement membranes, is thought to be crucial for basement assembly, by connecting the major networks formed by laminins and collagen IV (Fox et al., 1991). The nidogen-binding site of laminin has been localized to a single laminin-type epidermal growth factor-like (LE) module, γ1III4, of the laminin γ1 chain (Mayer et al., 1993) and is, therefore, present in most of the laminin isoforms known. Thus, it is possible that the laminin-type epidermal growth factor-like domain in the ORF022R may play some role in cell-to-cell adhesion in virus-infected cells and possibly this cell-to-cell interaction may support the rapid spreading of the virus from cell to cell. Cell-to-cell spread appears to be especially important in the spread of a progeny virus to neighboring cells while protecting the progeny virus from host enzymes and antibodies, especially after reactivation in hosts that have fully primed immunity. Consistent with this, HSV, PRV, and VZV all remain largely cell associated; many progeny virions accumulate on cell surfaces, especially at cell junctions in polarized epithelial cells (Johnson et al., 2001).

Three ORFs, such as ORF092R, ORF107L, and ORF113L encoded proteins which contain ankyrin repeats.

Ankyrin-like repeats are found in diverse proteins, including those with roles in transcription, the cell cycle, and tissue differentiation (Bork, 1993; Lux et al., 1990), and are believed to mediate protein–protein interactions (Bennett, 1992). Many large viruses that encode ankyrin repeat genes have been associated with host functions. An

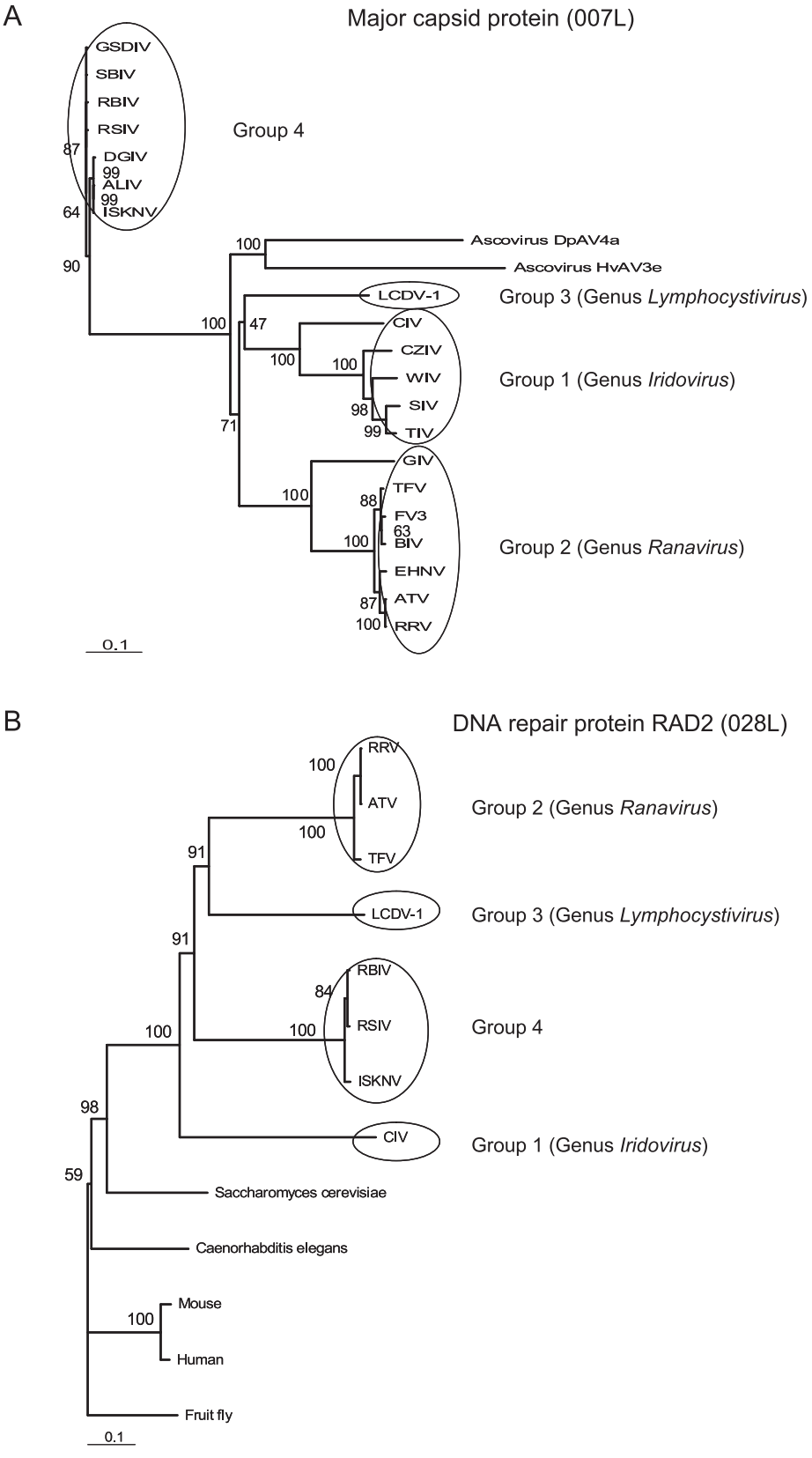

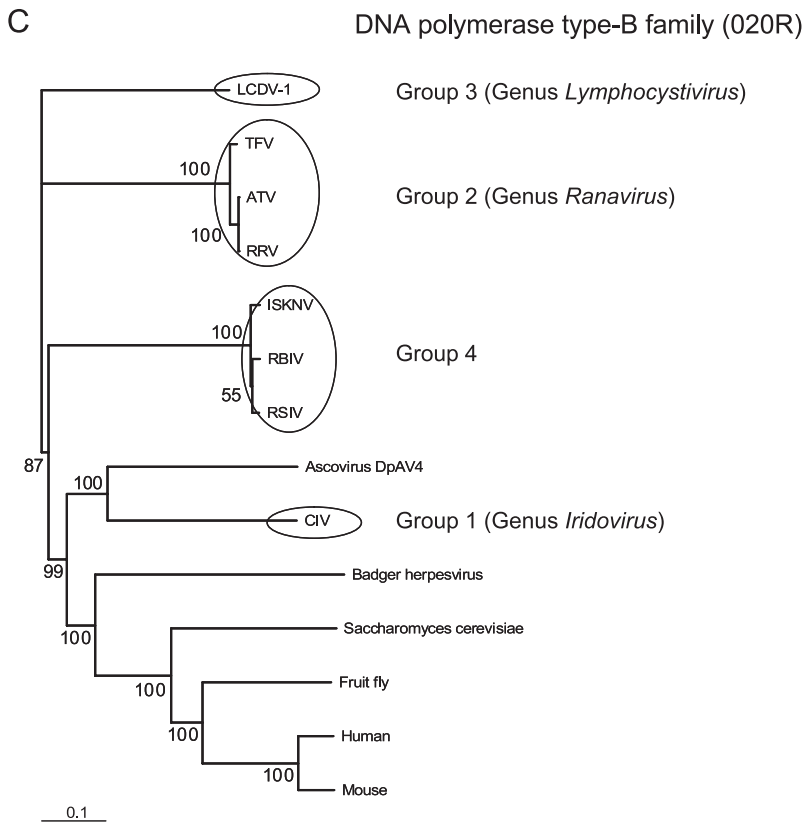

Fig. 2. Phylogenetic relationships of iridoviruses obtained using three protein sequence alignments: (A) major capsid protein, (B) DNA repair protein RAD2, (C) DNA polymerase type-B family. Predicted amino acid sequences of a 163-aa region of the RBIV MCP were compared with those from 19 iridoviruses. GenBank accession numbers for protein sequences are as follows: African lampeye iridovirus (ALIV) AAP37442; Ascovirus DpAV4 CAC19127; *Ambystoma tigrinum* virus (ATV) AAP33191, AAP33187, AAP33223; badger herpesvirus AAM62282; bohle iridovirus (BIV) AAO32316; *Caenorhabditis elegans* NP_491168; *Chilo* iridescent virus (CIV) NP_149737, AAK82229, NP_149500; *Costelytra zealandica* iridescent virus (CZIV) O39164; *Diadromus pulchellus* ascovirus 4a (Ascovirus DpAV4a) CAC84483; dwarf gourami iridovirus (DGIV) AAP37441; epizootic haematopoietic necrosis virus (EHNV) AAO32315; fruit fly NP_523765, NP_524099; frog virus 3 (FV3) Q67473; grouper iridovirus (GIV) AAM00286; grouper sleepy disease iridovirus (GSDIV) AAP37443; *Heliotis virescens* ascovirus 3e (Ascovirus HvAV3e) CAF05814; human NP_004102, NP_002682; infectious spleen and kidney necrosis virus (ISKNV) NP_612228, NP_612249, NP_612241; lymphocystis disease virus 1 (LCDV-1) NP_044812, NP_078767, NP_078724; mouse P39749, AAB99910; Regina ranavirus (RRV) YP_003785, YP_003781, YP_003817; red sea bream iridovirus (RSIV) BAC66968, BAA82754, BAA28669; *Saccharomyces cerevisiae* NP_012809, CAA43922; sea bass iridovirus (SBIV) BAC77297; Simulium iridescent virus (SIV) P22166; tiger frog iridovirus (TFV) NP_572010, NP_572012, NP_572000; Tipula iridescent virus (TIV) P18162; Wiseana iridescent virus (WIV)O39163. The numbers indicate the percentage bootstrap support for each node from 1000 replicates. The distances are proportional to the relative sequence deviations between individual amino acid sequences. The phylogenetic analyses were carried out with the ClustalW program.

ankyrin repeats gene of the cowpox virus, CHOhr, was found to inhibit virus-induced apoptosis (Ink et al., 1995). African swine fever virus encodes a protein of 28.2 kDa containing ankyrin repeats similar to those of cellular IκB proteins and this IκB gene homologue interferes with NF-κB activation, likely representing a new mechanism to evade the immune response during viral infection (Revilla et al., 1998). Similarly, RBIV ankyrin repeats genes may play some role in the control of the functions of viral and cellular proteins.

Protein encoded by ORF099L showed homology to the TRAF2. TRAF2 molecule serves as an adapter protein that links TNF receptors and downstream kinase cascades, which results in an activation of NF-κB and JNK (Rothe et al., 1995). The TRAF2 protein consists of a conserved C-terminal TRAF domain and an N-terminal region containing a RING-finger motif and an additional array of zinc-finger-like structures (Cheng et al., 1995; Hu et al., 1994; Rothe et al., 1994). The TRAF domain is involved in receptor association and homo- and hetero-oligomerization of TRAFs and serves as a docking site for several other signaling proteins (Cheng et al., 1995; Hu et al., 1994; Rothe et al., 1994). The N-terminal RING and zinc-finger motifs are important for signaling downstream events (Dadgostar and Cheng, 1998). RBIV ORF099L has the TRAF2 domain at its C-terminus and RING-finger motif at the N-terminus which may play some role in the control of the activation of the NF-κB and JNK in virus-infected cells.

RBIV also encodes proteins homologous to putative phosphatase (ORF022L) and ATPase (ORF116R).

Structural RBIV virion proteins

ORF007L encoded a protein of 453 amino acids which showed similarity to the major capsid proteins (MCP) of other iridoviruses (i.e., RSIV, DGIV, ALIV, SBIV, GSDIV, and ISKNV) (He et al., 2001; Sudthongkong et al., 2002). MCP is the predominant structural component of the virus particles, comprising 40–50% of the total particle polypeptide. It is a late gene product and its expression appears to be translationally regulated in the iridoviruses (Williams, 1996). RBIV is a large DNA virus and it is possible to possess more than one structural protein. For example, fowlpox virus encodes homologues of at least 31 structural proteins (Afonso et al., 2000). Further study of the structure of iridoviruses will reveal more structural proteins.

Phylogenetic analysis of the sequence of RBIV

To determine the relationship between RBIV and previous reported iridoviruses, we compared the full amino acid sequences for the major capsid protein (ORF007L), DNA repair protein RAD2 (ORF028L), and DNA polymerase type-B family (ORF020R), with those of other iridoviruses, non-iridoviruses, and eukaryotic organisms available in GenBank. In the MCP tree, the iridoviruses used in the multiple alignments were subdivided into four groups (Fig. 2A): group 1, iridoviruses including CIV (type species of Genus *Iridovirus*), CZIV, SIV, TIV, and WIV; group 2, ranaviruses including FV3 (type species of Genus *Ranavirus*), GIV, EHNV, TFV, ATV, BIV, and RRV; group 3, lymphocystiviruses including LCDV-1 (type species of Genus *Lymphocystivirus*); group 4, unassigned viruses including RBIV, ISKNV, DGIV, ALIV, SBIV, GSDIV, and RSIV. Phylogenetic trees for DNA repair protein RAD2 and DNA polymerase type-B family also yielded four groups within the Family *Iridoviridae* (Figs. 2B and C). Hyatt et al. (2000) suggested the presence of two groups of iridoviruses which are not closely related to any of the known genus. Although it is not certain whether group 4 is the same ones as one of those suggested by Hyatt et al. (2000), our analysis also supports the possibility of the presence of at least one more distinct group in the family Iridoviridae. The RBIV sequence segregated into group 4 which does not include any of the three type species. This result suggests that RBIV is not closely related to any of the previously characterized genus of the iridovirus and forms a distinct group within the family Iridoviridae, a new genus, tentatively called the cell hypertrophy iridoviruses suggested by He et al. (2001).

Conclusion

The genome sequence of RBIV has been determined. The genomic organization, gene content, and amino acid composition of RBIV are very similar to those of ISKNV but different from those of LCDV-1, which indicates a close structural and functional relationship between RBIV and ISKNV. The phylogeny on major capsid protein, DNA repair protein RAD2, and DNA polymerase type-B family strongly suggests that RBIV is a member of a new group which includes ISKNV and RSIV. Although the RBIV genome is very similar to the ISKNV genome, sharing colinearity (85 orthologous genes), relatively low amino acid identities exist among 32 genes (60–90% amino acid identity) and these low identities may be the result of the virus–host specificity. An improved understanding of RBIV–host interactions will have a broad impact on future strategies for controlling iridoviral disease in cultured fish.

Materials and methods

Virus DNA isolation

The virus sample used in this study was obtained from moribund rock bream cultured at a fish farm in Tongyeong area located at southern part of Korean peninsular during epizootics in 2000. The grunt fin (GF) cells were grown at 25 °C in Basal Medium Eagle (BME) supplemented with 10% fetal bovine serum, 100 IU/ml penicillin, and 100 μg/ml streptomycin. Virus stocks were amplified by an infection of the GF cells. Infected cells showing cytopathic effects (CPE) were collected and frozen at −20 °C. Frozen cells with CPE were thawed, cell debris was taken out at 3500 × *g* for 10 min at 4 °C, and the cell-free supernatant was centrifuged at 30 000 × *g* for 30 min at 4 °C. The virus pellet was resuspended with TNE buffer (0.01 M Tris–HCl, pH 8.0, 0.1 M NaCl, 0.001 M EDTA) and incubated with DNase I and RNase A at 37 °C for 15 min. The virus was purified by centrifugation at 60 000 × *g* for 2 h at 4 °C in a SW40 Ti rotor (Beckman) through 20–50% (w/w) sucrose gradients. The viral band was removed and diluted with PBS buffer, and the virion pellets were collected after 1 h of centrifugation at 60 000 × *g* at 4 °C. Virus DNA was extracted by incubating virions with 0.5 mg/ml proteinase K and 0.5% SDS at 55 °C for 3 h. The DNA was then subjected to phenol–chloroform extraction and ethanol precipitation (Sambrook et al., 1989).

PCR amplification of viral DNA and DNA sequencing

PCR was performed to amplify complete genomic DNA of RBIV. Primers for PCR were designed from nucleotide sequences in the GenBank/EMBL databases of ISKNV (AF371960). More than overlapping 120 PCR primer pairs were designed so that the average PCR product ranged from 1000 to 1200 bp. The template was the genomic DNA of RBIV. The gene amplification reaction conditions were as follows: 1 cycle of 94 °C for 5 min; 35 cycles of 92 °C for 30 s, 60 °C for 1 min, and 72 °C for 1 min; and 1 cycle of 72 °C for 5 min. There were some variations in the

annealing temperature depending on the PCR primer sets. The amplified PCR products were cloned into pGEM-T vector (Promega), and sequencing was performed at the Immunomodulation Research Center, Korea, on an automatic DNA sequencer (Applied Biosystems, Inc., USA) according to the dye terminator procedure with forward and reverse primers and overlapping primers designed from the sequencing results.

DNA sequence analysis

The DNA and the deduced amino acid sequences were compared with the GenBank/EMBL databases using BLAST. Sequences were aligned using CLUSTAL W (Thompson et al., 1994) and then the phylogenetic tree was constructed with the TreeView (Page, 1996). The phylogenetic relationships among species were determined using the neighbor-joining method (NJ; Saitou and Nei, 1987) and the reliability of the NJ tree was inferred using the Felsenstein (1985) bootstrap method with 1000 replicates.

ORFs were identified by the following criteria: they consisted of more than 50 codons that are initiated with a methionine codon and they were not located within larger ORFs.

Nucleotide sequence accession number

The nucleotide sequence data reported in this paper were deposited to the GenBank as accession number AY532606.

Acknowledgments

This study was supported by a grant from National Fisheries Research and Development Institute. Hyo Jeong Kim and Jong Soo Kim were partly supported by the BK21 program of the Korea Research Foundation.

References

Afonso, C.L., Tulman, E.R., Lu, Z., Zsak, L., Kutish, G.F., Rock, D.L., 2000. The genome of Fowlpox virus. J. Virol. 74, 3815–3831.

Ahne, W., Schlotfeldt, H.J., Thomsen, I., 1989. Fish viruses: isolation of an icosahedral cytoplasmic deoxyribovirus from sheatfish (*Silurus glanis*). J. Vet. Med. 36, 333–336.

Bennett, V., 1992. Ankyrins: adaptors between diverse plasma membrane proteins and the cytoplasm. J. Biol. Chem. 267, 8703–8706.

Bork, P., 1993. Hundreds of ankyrin-like repeats in functionally diverse proteins: mobile modules that cross phyla horizontally. Protein Struct.-Funct. Genet. 17, 363–374.

Cheng, G., Cleary, A.M., Ye, Z.-S., Hong, D., Lederman, S., Baltimore, D., 1995. Involvement of CRAF1, a relative of TRAF, in CD40 signaling. Science 267, 1494–1498.

Cunningham, C., Davison, A.J., Dolan, A., Frame, M.C., McGeoch, D.J., Meredith, D.M., Moss, H.W., Orr, A.C., 1992. The UL13 virion protein of herpes simplex virus type 1 is phosphorylated by a novel virus-induced protein kinase. J. Gen. Virol. 73, 303–311.

Dadgostar, H., Cheng, G., 1998. An intact zinc ring finger is required for tumor necrosis factor receptor-associated factor-mediated nuclear factor-kappaB activation but is dispensable for c-Jun N-terminal kinase signaling. J. Biol. Chem. 273, 24775–24780.

Everett, R.D., 1988. Analysis of the functional domains of herpes simplex virus type 1 immediate-early polypeptide Vmw110. J. Mol. Biol. 202, 87–96.

Everett, R.D., 2000. ICP0 induces the accumulation of conjugated ubiquitin. J. Virol. 74, 9994–10005.

Felsenstein, J., 1985. Confidence limits on phylogenies: an approach using bootstrap. Evolution 39, 783–791.

Fox, J.W., Mayer, U., Nischt, R., Aumailley, M., Reinhardt, D., Wiedemann, H., Mann, K., Timpl, R., Krieg, T., Engel, J., Timpl, R., 1991. Recombinant nidogen consists of three globular domains and mediates binding of laminin to collagen type IV. EMBO J. 10, 3137–3146.

Goorha, R., Murti, K.G., 1982. The genome of frog virus 3, an animal DNA virus, is circularly permuted and terminally redundant. Proc. Natl. Acad. Sci. U.S.A. 79, 248–252.

He, J.G., Deng, M., Weng, S.P., Li, Z., Zhou, S.Y., Long, Q.X., Wang, X.Z., Chan, S.M., 2001. Complete genome analysis of the mandarin fish infectious spleen and kidney necrosis iridovirus. Virology 291, 126–139.

He, J.G., Lu, L., Deng, M., He, H.H., Weng, S.P., Wang, X.H., Zhou, S.Y., Long, Q.X., Wang, X.Z., Chan, S.M., 2002. Sequence analysis of the complete genome of an iridovirus isolated from the tiger frog. Virology 292, 185–197.

Hedrick, R.P., McDowell, T.S., 1995. Properties of iridoviruses from ornamental fish. Vet. Res. 26, 423–427.

Hedrick, R.P., McDowell, T.S., Ahne, W., Torhy, C., de Kinkelin, P., 1992. Properties of three iridovirus-like agents associated with systemic infections of fish. Dis. Aquat. Org. 13, 203–209.

Hetrick, F.M., Hedrick, R.P., 1993. New viruses described in finfish from 1988–1992. Annu. Rev. Fish Dis. 3, 187–207.

Hu, H.M., O'Rourke, K., Boguski, M.S., Dixit, V.M., 1994. A novel RING finger protein interacts with the cytoplasmic domain of CD40. J. Biol. Chem. 269, 30069–30072.

Hyatt, A.D., Gould, A.R., Zupanovic, Z., Cunningham, A.A., Hengstberger, S., Whittington, R.J., Kattenbelt, J., Coupar, B.E., 2000. Comparative studies of piscine and amphibian iridoviruses. Arch. Virol. 145, 301–331.

Ink, B.S., Gilbert, C.S., Evan, G.I., 1995. Delay of vaccinia virus-induced apoptosis in nonpermissive Chinese hamster ovary cells by the cowpox virus CHOhr and adenovirus E1B 19K genes. J. Virol. 69, 661–668.

Jakob, N.J., Muller, K., Bahr, U., Darai, G., 2001. Analysis of the first complete DNA sequence of an invertebrate iridovirus: coding strategy of the genome of Chilo iridescent virus. Virology 286, 182–196.

Jancovich, J.K., Mao, J., Chinchar, V.G., Wyatt, C., Case, S.T., Kumar, S., Valente, G., Subramanian, S., Davidson, E.W., Collins, J.P., Jacobs, B.L., 2003. Genomic sequence of a ranavirus (family *Iridoviridae*) associated with salamander mortalities in North America. Virology 316, 90–103.

Johansson, K., Ramaswamy, S., Ljungcrantz, C., Knecht, W., Piškur, J., Munch-Petersen, B., Eriksson, S., Eklund, H., 2001. Structural basis for substrate specificities of cellular deoxyribonucleoside kinases. Nat. Struct. Biol. 8, 616–620.

Johnson, D.C., Webb, M., Wisner, T.W., Brunetti, C., 2001. Herpes simplex virus gE/gI sorts nascent virions to epithelial cell junctions, promoting virus spread. J. Virol. 75, 821–833.

Jung, S.J., Oh, M.J., 2000. Iridovirus-like infection associated with high mortalities of striped beakperch, *Oplegnathus fasciatus* (Temmink et Schlegel), in southern coastal areas of the Korean peninsula. J. Fish Dis. 23, 223–226.

Kim, Y.J., Jung, S.J., Choi, T.J., Kim, H.R., Rajendran, K.V., Oh, M.J., 2002. PCR amplification and sequence analysis of irido-like virus infecting fish in Korea. J. Fish Dis. 25, 121–124.

Knecht, W., Munch-Petersen, B., Piškur, J., 2000. Identification of residues involved in the specificity and regulation of the highly efficient

multisubstrate deoxyribonucleoside kinase from *Drosophila melanogaster*. J. Mol. Biol. 301, 827–837.

Langdon, J.S., Humphrey, J.D., Williams, L.M., Hyatt, A.D., Westbury, H.A., 1986. First virus isolation from Australian fish: an iridovirus-like pathogen from redfin perch *Perca fluviatilis*. J. Fish Dis. 9, 263–268.

Lux, S.E., John, K.M., Bennett, V., 1990. Analysis of cDNA for human erythrocyte ankyrin indicates a repeated structure with homology to tissue-differentiation and cell-cycle control proteins. Nature 433, 36–42.

Mayer, U., Nischt, R., Pöschl, E., Mann, K., Fukuda, K., Gerl, M., Yamada, Y., Timpl, R., 1993. A single EGF-like motif of laminin is responsible for high affinity nidogen binding. EMBO J. 12, 1879–1885.

O'Brien, T., Hardin, S., Greenleaf, A., Lis, J.T., 1994. Phosphorylation of RNA polymerase II C-terminal domain and transcriptional elongation. Nature 370, 75–77.

Overton, H.A., McMillan, D.J., Klavinskis, L.S., Hope, L., Ritchie, A.J., Wong-kai-in, P., 1992. Herpes simplex virus type 1 gene UL13 encodes a phosphoprotein that is a component of the virion. Virology 190, 184–192.

Page, R.D., 1996. TreeView: an application to display phylogenetic trees on personal computers. Comput. Appl. Biosci. 12, 357–358.

Pozet, F., Morand, M., Moussa, A., Torhy, C., de Kinkelin, P., 1992. Isolation and preliminary characterization of a pathogenic icosahedral deoxyribovirus from the catfish *Ictalurus melas*. Dis. Aquat. Org. 14, 35–42.

Reichard, P., 1988. Interaction between the deoxyribonucleotide and DNA synthesis. Annu. Rev. Biochem. 57, 349–374.

Revilla, Y., Callejo, M., Rodriguez, J.M., Culebras, E., Nogal, M.L., Salas, M.L., Vinuela, E., Fresno, M., 1998. Inhibition of nuclear factor kappaB activation by a virus-encoded IkappaB-like protein. J. Biol. Chem. 273, 5405–5411.

Rothe, M., Wong, S.C., Henzel, W.J., Goeddel, D.V., 1994. A novel family of putative signal transducers associated with the cytoplasmic domain of the 75 kDa tumor necrosis factor receptor. Cell 78, 681–692.

Rothe, M., Sarma, V., Dixit, V.M., Goeddel, D.V., 1995. TRAF2-mediated activation of NF-kappa B by TNF receptor 2 and CD40. Science 269, 1424–1427.

Saitou, N., Nei, M., 1987. The neighbor-joining method: a new method for reconstructing phylogenetic trees. Mol. Biol. Evol. 4, 406–425.

Sambrook, J., Fritsch, E.F., Maniatis, T., 1989. Molecular Cloning: A Laboratory Manual Cold Spring Harbor Laboratory Press, Cold Spring Harbor, NY.

Sudthongkong, C., Miyata, M., Miyazaki, T., 2002. Viral DNA sequences of genes encoding the ATPase and the major capsid protein of tropical iridovirus isolates which are pathogenic to fishes in Japan, South China Sea and Southeast Asian countries. Arch. Virol. 147, 2089–2109.

Thompson, J.D., Higgins, D.G., Gibson, T.J., 1994. CLUSTAL W: improving the sensitivity of progressive multiple sequence alignment through sequence weighting, position-specific gap penalties and weight matrix choice. Nucleic Acids Res. 22, 4673–4680.

Tidona, C.A., Darai, G., 1997. The complete DNA sequence of lymphocystis disease virus. Virology 230, 207–216.

Williams, T., 1996. The iridoviruses. Adv. Virus Res. 46, 345–412.

Wolf, K., 1988. Fish Viruses and Fish Viral Diseases Cornell Univ. Press, Ithaca.